Indian J. pure appl. Math., 27(9) : 913-929, September 1996

DISCRETE WAVE NUMBER REPRESENTATION OF SEISMIC SOURCE WAVE FIELDS IN FLUID SATURATED POROUS MEDIA

M. D. SHARMA AND M. L. GOGNA

Department of Mathematics, Kurukshetra University, Kurukshetra 132 119

(*Received* 3 *July* 1995; *after revision* 30 *January* 1996; *accepted* 22 *March* 1996)

A method based on the discrete wave number representation of seismic source wave-fields is applied to investigate the near-field of a seismic source, embedded in a fluid saturated porous solid. Seismic source is assumed to be either (i) a vertical line force or (ii) a horizontal line force. Analytical expressions in the form of converging infinite series are obtained for the exact evaluation of displacements at the free surface of a fluid saturated porous medium. Similar expressions for ordinary elastic medium are also obtained. To analyse the effects of porosity, an elasticity of the solid, and viscosity of the interstitial fluid, synthetic seismograms are computed for six particular media. Arrival of P and S waves at the recording station and variations in their amplitudes are discussed.

INTRODUCTION

The presence of pores and microcracks in the crustal rocks have been recognized for some time. Recent studies suggest that water is contained in the pore space of sedimentary rocks when they are first deposited (Crampin[7]). Crampin[8] has explained that pore fluid plays an important role in the preparation of earthquakes.

Biot[2] developed a theory to explain the wave propagation in fluid saturated porous materials. These materials consist of a porous assemblage of sediment grains whose interconnected pores are filled with liquid or gas. Deresiewicz and Skalak[9] derived the boundary conditions appropriate for the continuity requirements at the interface of such materials. Burridge and Vargas[6], Paul[12, 13] and Norris[11] studied the problems concerning the waves produced by impulsive loads in such solids. Boutin *et al.*[5] studied the Green functions for porous saturated media by applying the results of homogenization theory developed by Aurialt[1]. In recent years, a lot of work has been done on various aspects of wave propagation in poroelastic media but very few of these addressed the source problems. Philippacopoulos[14] discussed the axisymmetric wave propagation in a fluid saturated porous solid half-space. Sharma[15] changed the boundary conditions used by Philippacopoulos[14] to satisfy the basic concept of porosity and derived the corrected analytical expressions for displacements at the surface.

In order to contibute towards the development of strong motion seismology, Bouchon and Aki[4] presented a reliable numerical technique which gives the workable exact solutions of seismic source problems. Basic idea is to represent the source as a superposition of homogeneous and inhomogeneous plane waves propagating at discrete angles. This technique assumes a periodic description of the source and considers an infinite number of such sources distributed in a striaght line at equal intervals. The distance between the sources is assumed such that perturbations from the neighbouring sources reach the surface after the time interval of interest. In many seismic regions, instruments have been installed close-in along known active faults. These installations provide data from areas in the immediate neighbourhood of shallow earthquake sources. The analysis of these data requires the solution of source radiation problems in the near-field. The wave number discretization method presented by Bouchon and Aki[4] is applicable, specially, to study the near-field of a seismic source.

In this work, we propose to apply this method to study the near-field of a seismic source embedded in a fluid saturated porous solid half-space. Synthetic seismograms are computed numerically for some theoretical models. This study assumes importance when we think of the variations in particle motion (in an earthquake preparation region) as a possible precursor for earthquake prediction.

FIELD EQUATIONS AND THEIR SOLUTIONS

Following Biot[3], the differential equations governing the displacement $\vec{u}$ of the solid matrix and $\vec{U}$ of the interstitial fluid, in a homogeneous isotropic poroelastic solid, are

$$\left.\begin{aligned} \mu\nabla^2\vec{u} + (\lambda+\mu+\alpha^2 M)\,\mathrm{grad}\,(\nabla\cdot\vec{u}) + \alpha M\,\mathrm{grad}\,(\nabla\cdot\vec{w}) &= \frac{\partial^2}{\partial t^2}(\rho\,\vec{u} + \rho_f\vec{w}) \\ \mathrm{grad}\,[\alpha M(\nabla\cdot\vec{u}) + M(\nabla\cdot\vec{w})] &= \frac{\partial^2}{\partial t^2}(\rho_f\vec{u} + m\,\vec{w}) + \frac{\eta}{\kappa}\frac{\partial\vec{w}}{\partial t}. \end{aligned}\right\} \quad \dots (1)$$

The vector $\vec{w}$ $\{=\beta(\vec{U}-\vec{u})\}$ represents the flow of fluid relative to the solid measured in terms of volume per unit area of the bulk medium. Other parameters in eqations (1) are defined as follows :

λ, μ = Lame's constants for the solid;

ρ, ρ_f = mass densities of the bulk material and fluid respectively;

m = Biot's parameter which depends upon porosity β and ρ_f;

η = pore fluid viscosity; and

κ = permeability.

α and M are elastic coefficients related to the coefficients of fluid viscosity γ, unjacketed compressibility δ and jacketed incompressibility $K\,(=\lambda + 2\mu/3)$ by

$$\left.\begin{aligned} \alpha &= 1-\delta K \\ M &= 1/(\gamma+\delta-\delta^2 K) \end{aligned}\right\} \qquad \ldots (2)$$

In poroelastic media, the stress components τ_{ij}, in the bulk material and the fluid pressure, P_f, are given by

$$\left.\begin{aligned} \tau_{ij} &= 2\mu\, e_{ij} + \left\{ (\lambda+\alpha^2 M)e + \alpha M \xi \right\} \delta_{ij}\,,; \quad (i, j = x, y, z) \\ P_f &= -\alpha M e - M\xi \end{aligned}\right\} \qquad \ldots (3)$$

where $e = \text{div}\ \vec{u}$, $\xi = \text{div}\ \vec{w}$ and $e_{ij} = \frac{1}{2}(u_{i,j} + u_{j,i})$.

Solving eqns. (1) for time harmonic excitations ($\sim e^{i\omega t}$), we get

$$\left.\begin{aligned} \vec{u} &= \text{grad}\ \phi_1 + \text{grad}\ \phi_2 + \text{curl}\ \vec{\psi_1} \\ \vec{w} &= \mu_1\, \text{grad}\ \phi_1 + \mu_2\, \text{grad}\ \phi_2 + \mu_3\, \text{curl}\ \vec{\psi_1} \end{aligned}\right\} \qquad \ldots (4)$$

where the potentials ϕ_1, ϕ_2 and $\vec{\psi_1}$ satisfy the Helmholtz equations, given by

$$\left(\nabla^2 + \frac{\omega^2}{v_k^2}\right)\phi_k = 0; \quad (k = 1,\ 2) \qquad \ldots (5a)$$

$$\left(\nabla^2 + \frac{\omega^2}{v_3^2}\right)\vec{\psi_1} = 0. \qquad \ldots (5b)$$

If we define

$$\left.\begin{aligned} A &= (\lambda+2\mu)\, M\,; \\ H &= \lambda + 2\mu + \alpha^2 M\,; \\ B &= \rho M + \left(m - i\frac{\eta}{\omega\chi}\right) H - 2\rho_f\, \alpha M\,; \\ C &= \rho\left(m - i\frac{\eta}{\omega\chi}\right) - \rho_f^2\,; \\ \rho_k &= \frac{B + (-1)^k \sqrt{B^2 - 4AC}}{2M}\,, \quad (k = 1, 2); \\ \rho_3 &= C \Big/ \left(m - i\frac{\eta}{\omega\chi}\right), \end{aligned}\right] \qquad \ldots (6)$$

the velocities, v_k, are given by

$$v_k^2 = (\lambda + 2\mu)/\rho_k, \quad (k = 1, 2); \qquad v_3^2 = \mu/\rho_3 . \qquad \text{... (7)}$$

The constant μ_1, μ_2 and μ_3 in equations (4) are defined as :

$$\mu_k = \frac{\rho_f \alpha - \rho + \rho_k}{\rho_f - \left(m - i\dfrac{\eta}{\omega\chi}\right)\alpha}, \ (k = 1, 2); \quad \mu_3 = -\frac{\rho_f}{\left(m - i\dfrac{\eta}{\omega\chi}\right)} . \qquad \text{... (8)}$$

WAVE POTENTIALS

For two-dimensional motion in the x–z plane, the solutions of eqns. (5) are considered as

$$\phi_j = A_j e^{a_j z - ikx} + B_j e^{-a_j z - ikx}, \quad (j = 1, 2, 3) \qquad \text{... (9)}$$

where

$$\phi_3 = (\vec{\psi}_1)_y, \text{ and } a_j = \sqrt{k^2 - \omega^2/v_j^2}, \ (j = 1, 2, 3).$$

Expressions for the displacement components reduce to

$$\left.\begin{aligned} u_x &= \frac{\partial\phi_1}{\partial x} + \frac{\partial\phi_2}{\partial x} + \frac{\partial\phi_3}{\partial z} ; \quad w_x = \mu_1\frac{\partial\phi_1}{\partial x} + \mu_2\frac{\partial\phi_2}{\partial x} + \mu_3\frac{\partial\phi_3}{\partial z} ; \\ u_z &= \frac{\partial\phi_1}{\partial z} + \frac{\partial\phi_2}{\partial z} - \frac{\partial\phi_3}{\partial x} ; \quad w_z = \mu_1\frac{\partial\phi_1}{\partial z} + \mu_2\frac{\partial\phi_2}{\partial z} - \mu_3\frac{\partial\phi_3}{\partial x} . \end{aligned}\right] \qquad \text{... (10)}$$

BOUNDARY VALUE PROBLEMS

We shall first derive expressions for the wave fields associated with a vertical force. For a two-dimensional motion in the x-z plane we consider an internal vertical line force $Q_v e^{i\omega t}$, applied at (x_0, z_0), acting in the positive z-direction. Following Lamb[10] and Deresiewicz and Skalak[9], the boundary conditions, involving a normal periodic force $Y_v e^{-ik(x-x_0)}$ per unit area acting at the plane $z = z_0$, are

$$\left.\begin{aligned} &\text{(i)} && \tau_{zz}|_{z_0^+} - \tau_{zz}|_{z_0^-} = -Y_v \exp\{-ik(x-x_0)\} \\ &\text{(ii)} && \tau_{zx}|_{z_0^+} - \tau_{zx}|_{z_0^-} = 0, \\ &\text{(iii)} && P_f|_{z_0^+} - P_f|_{z_0^-} = Y_v \exp\{-ik(x-x_0)\} \\ &\text{(iv)} && u_x|_{z_0^+} - u_x|_{z_0^-} = 0, \\ &\text{(v)} && u_z|_{z_0^+} - u_z|_{z_0^-} = 0, \\ &\text{(vi)} && w_z|_{z_0^+} - w_z|_{z_0^-} = 0. \end{aligned}\right] \qquad \text{... (11)}$$

The source potentials satisfying the above conditions are found to be

$$\left.\begin{aligned}\phi_1 &= \operatorname{sgn}(z-z_0)\frac{Y_v}{2(\lambda+2\mu)}\frac{R_2}{\delta_1^2}\exp\{-a_1|z-z_0|-ik(x-x_0)\}\\ \phi_2 &= -\operatorname{sgn}(z-z_0)\frac{Y_v}{2(\lambda+2\mu)}\frac{R_1}{\delta_2^2}\exp\{-a_2|z-z_0|-ik(x-x_0)\}\\ \phi_3 &= -\frac{ik}{a_3}\frac{Y_v}{2(\lambda+2\mu)}\left(\frac{R_2}{\delta_1^2}-\frac{R_1}{\delta_2^2}\right)\exp\{-a_3|z-z_0|-ik(x-x_0)\}\end{aligned}\right] \quad \ldots (12)$$

where

$$\left.\begin{aligned}&\delta_k^2 = \omega^2/v_k^2, \quad (k=1,2,3), \text{ and}\\ &R_k = \frac{1}{(\mu_1-\mu_2)}\left\{\frac{(\lambda+2\mu)}{M}+(\alpha-1)(\alpha+\mu_k)\right\}, \quad (k=1,2).\end{aligned}\right] \quad \ldots (13)$$

A vertical line force $Q_v e^{i\omega t}$ can be obtained by superposing the infinite number of stress distributions, given by (11), with every possible wave number k. Hence the source potentials for an internal vertical line force $Q_v e^{i\omega t}$, applied at (x_0, z_0) in the positive z-direction, are

$$\phi_1 = \operatorname{sgn}(z-z_0)\frac{Q_v}{4\pi(\lambda+2\mu)}\frac{R_2}{\delta_1^2}\int_{-\infty}^{+\infty}\exp\{-a_1|z-z_0|-ik(x-x_0)\}\,dk$$

$$\phi_2 = -\operatorname{sgn}(z-z_0)\frac{Q_v}{4\pi(\lambda+2\mu)}\frac{R_1}{\delta_2^2}\int_{-\infty}^{+\infty}\exp\{-a_2|z-z_0|-ik(x-x_0)\}\,dk$$

... (14)

$$\phi_3 = \frac{Q_v}{4\pi(\lambda+2\mu)}\left(\frac{R_2}{\delta_1^2}-\frac{R_1}{\delta_2^2}\right)\int_{-\infty}^{+\infty}\left\{\frac{-ik}{a_3}\right\}\exp\{-a_3|z-z_0|-ik(x-x_0)\}dk.$$

Following Bouchon and Aki[4], we consider an infinite number of such sources distributed along the horizontal x-axis, at equal interval L. The source potentials in this case will reduce to

$$\phi_1 = \operatorname{sgn}(z-z_0)\frac{Q_v}{2L(\lambda+2\mu)}\frac{R_2}{\delta_1^2}\sum_{n=-N}^{N}\exp\{-\alpha_n|z-z_0|-ik_n(x-x_0)\}$$

... (15a)

$$\phi_2 = -\operatorname{sgn}(z-z_0)\frac{Q_v}{2L(\lambda+2\mu)}\frac{R_1}{\delta_2^2}\sum_{n=-N}^{N}\exp\{-\beta_n|z-z_0|-ik_n(x-x_0)\}$$

... (15b)

$$\phi_3 = \frac{Q_v}{2L(\lambda+2\mu)}\left(\frac{R_2}{\delta_1^2}-\frac{R_1}{\delta_2^2}\right)\sum_{n=-N}^{N}\left(-i\frac{k_n}{\gamma_n}\right)\exp\{-\gamma_n|z-z_0|-ik_n(x-x_0)\}$$

... (15c)

where

$$\left.\begin{aligned}\alpha_n &= \sqrt{(k_n^2-\delta_1^2)}\ ;\quad \mathrm{Re}(\alpha_n)>0\,,\\ \beta_n &= \sqrt{(k_n^2-\delta_2^2)}\ ;\quad \mathrm{Re}(\beta_n)>0\,,\\ \gamma_n &= \sqrt{(k_n^2-\delta_3^2)}\ ;\quad \mathrm{Re}(\gamma_n)>0\,,\quad \text{and}\quad k_n=\frac{2\pi}{L}n.\end{aligned}\right] \quad \text{... (16)}$$

N is a positive integer chosen to approximate the sum of the infinite series.

Reflection at the Free Surface

Solving the stress free boundary conditions at the surface $z = 0$, yield the wave potentials :

$$\phi_1 = \varepsilon\sum_{n=-N}^{N}\left\{-\frac{R_2}{\delta_1^2}\exp\{\alpha_n(z-z_0)\}+\frac{F_{1n}}{F_n}e^{-\alpha_n z}\right\}\exp\{-ik_n(x-x_0)\}, \quad \text{... (17a)}$$

$$\phi_2 = \varepsilon\sum_{n=-N}^{N}\left\{\frac{R_1}{\delta_2^2}\exp\{\beta_n(z-z_0)\}-\frac{F_{2n}}{F_n}e^{-\beta_n z}\right\}\exp\{-ik_n(x-x_0)\}, \quad \text{... (17b)}$$

$$\phi_3 = -i\varepsilon\sum_{n=-N}^{N}\left(\frac{k_n}{\gamma_n}\right)\left\{\left(\frac{R_2}{\delta_1^2}-\frac{R_1}{\delta_2^2}\right)e^{\gamma_n(z-z_0)}+\frac{F_{3n}}{F_n}e^{-\gamma_n z}\right\}\exp\{-ik_n(x-x_0)\},$$

... (17c)

where

$$F_n = (k_n^2+\gamma_n^2)(T_{1n}S_2-T_{2n}S_1)-4\mu k_n^2\gamma_n(\alpha_nS_2-\beta_nS_1) \quad \text{... (18a)}$$

$$F_{1n} = \{(k_n^2+\gamma_n^2)(T_{1n}S_2 - T_{2n}S_1) + 4\mu k_n^2\gamma_n(\alpha_n S_2 + \beta_n S_1)\}\ \frac{R_2}{\delta_1^2}e^{-\alpha_n z_0}$$

$$- 8\mu k_n^2\gamma_n\beta_n S_2\ \frac{R_1}{\delta_2^2}e^{-\beta_n z_0} - 4\mu k_n^2\{k_n^2+\gamma_n^2\}\left(\frac{R_2}{\delta_1^2}-\frac{R_1}{\delta_2^2}\right)S_2 e^{-\gamma_n z_0}\ ;$$

... (18b)

$$F_{2n} = \{(k_n^2+\gamma_n^2)(T_{1n}S_2 - T_{2n}S_1) - 4\mu k_n^2\gamma_n(\alpha_n S_2 + \beta_n S_1)\}\ \frac{R_1}{\delta_2^2}e^{-\beta_n z_0}$$

$$+ 8\mu k_n^2\gamma_n\alpha_n S_1\ \frac{R_2}{\delta_1^2}e^{-\alpha_n z_0} - 4\mu k_n^2\{k_n^2+\gamma_n^2\}\left(\frac{R_2}{\delta_1^2}-\frac{R_1}{\delta_2^2}\right)S_1 e^{-\gamma_n z_0}\ ;$$

... (18c)

$$F_{3n} = (T_{1n}S_2 - T_{2n}S_1)\,4\gamma_n\left(\alpha_n\frac{R_2}{\delta_1^2}e^{-\alpha_n z_0} - \beta_n\frac{R_1}{\delta_2^2}e^{-\beta_n z_0}\right)$$

$$- [\{T_{1n}S_2 - T_{2n}S_1\}\ \{k_n^2+\gamma_n^2\} + 4\mu k_n^2\gamma_n\ (\alpha_n S_2 - \beta_n S_1)]$$

$$\times\left(\frac{R_2}{\delta_1^2}-\frac{R_1}{\delta_2^2}\right)e^{-\gamma_n z_0}\ ; \qquad \text{... (18d)}$$

$$\varepsilon = \frac{Q_v}{2L(\lambda+2\mu)}\ ;\ S_j = (\alpha+\mu_j)(-\delta_j^2),\quad (j = 1,\ 2); \qquad \text{... (19)}$$

and $$T_{jn} = \{\lambda + 2\mu + \alpha M(\alpha+\mu_j)\}\ (-\delta_j^2) + 2\mu k_n^2,\quad (j = 1,\ 2). \qquad \text{... (20)}$$

Rearranging the series for positive index, the displacement components of solid particles at the interface $z = 0$, are

$$u_x^0 = \frac{Q_v}{L\mu}(S_1\delta_2^2 - S_2\delta_1^2)\,\mu\sum_{n=1}^{N}\frac{k_n}{F_n}\left[\left\{\alpha_n\frac{R_2}{\delta_1^2}e^{-\alpha_n z_0} - \beta_n\frac{R_1}{\delta_2^2}e^{-\beta_n z_0}\right\}4\gamma_n\right.$$

$$\left. - 2\ \{k_n^2+\gamma_n^2\}\left(\frac{R_2}{\delta_1^2}-\frac{R_1}{\delta_2^2}\right)e^{-\gamma_n z_0}\right]\sin\ \{k_n(x-x_0)\} \qquad \text{... (21)}$$

$$u_z^0 = \frac{Q_v}{L\mu}\frac{\mu\delta_3^2}{\lambda+2\mu}\left[\frac{-i}{\delta_3^2}\left(\frac{R_2}{\delta_1}e^{-i\delta_1 z_0} - \frac{R_1}{\delta_2}e^{-i\delta_2 z_0}\right)\right.$$

$$+ 2\sum_{n=1}^{N}\left\{\ \{T_{1n}S_2 - T_{2n}S_1\}\left(\alpha_n\frac{R_2}{\delta_1^2}e^{-\alpha_n z_0} - \beta_n\frac{R_1}{\delta_2^2}e^{-\beta_n z_0}\right)\right.$$

$$\left.\left. - 2\mu k_n^2\{\alpha_n S_2 - \beta_n S_1\}\left(\frac{R_2}{\delta_1^2}-\frac{R_1}{\delta_2^2}\right)e^{-\gamma_n z_0}\ \right]\frac{1}{F_n}\cos\ \{k_n(x-x_0)\}\right]$$

... (22)

Similar to the case of a vertical line force, we derive expressions of potentials and displacement components for the wave-fields associated with the horizontal line force $Q_h e^{i\omega t}$, applied at (x_0, z_0). The boundary conditions, involving the tangential periodic force $Y_h e^{ik(x-x_0)}$, per unit area, acting at the surface $z = z_0$, are

$$\left.\begin{array}{llll} \text{(i)} & \tau_{zz}|_{z_0^+} - \tau_{zz}|_{z_0^-} & = & 0, \\ \text{(ii)} & \tau_{zx}|_{z_0^+} - \tau_{zx}|_{z_0^-} & = & -Y_h e^{-ik(x-x_0)}, \\ \text{(iii)} & P_f|_{z_0^+} - P_f|_{z_0^-} & = & 0, \\ \text{(iv)} & u_x|_{z_0^+} - u_x|_{z_0^-} & = & 0, \\ \text{(v)} & u_z|_{z_0^+} - u_z|_{z_0^-} & = & 0, \\ \text{(vi)} & w_z|_{z_0^+} - w_z|_{z_0^-} & = & 0. \end{array}\right] \quad \ldots (23)$$

The source potentials for such a stress distributions are

$$\left.\begin{array}{l} \phi_1 = i\dfrac{Y_h}{2\mu}\dfrac{k}{a_1}\dfrac{\mu_3-\mu_2}{\mu_1-\mu_2}\dfrac{1}{\delta_3^2}\exp\{-a_1|z-z_0|-ik(x-x_0)\} \\ \phi_2 = -i\dfrac{Y_h}{2\mu}\dfrac{k}{a_2}\dfrac{\mu_3-\mu_1}{\mu_1-\mu_2}\dfrac{1}{\delta_3^2}\exp\{-a_2|z-z_0|-ik(x-x_0)\} \\ \phi_3 = \operatorname{sgn}(z-z_0)\dfrac{Y_h}{2\mu}\dfrac{1}{\delta_3^2}\exp\{-a_3|z-z_0|-ik(x-x_0)\}. \end{array}\right] \quad \ldots (24)$$

For an infinite number of horizontal line forces distributed along the x-axis, at equal intervals L, we get

$$\phi_1 = i\frac{Q_h}{2L\mu}\frac{\mu_3-\mu_2}{\mu_1-\mu_2}\frac{1}{\delta_3^2}\sum_{n=-N}^{N}\frac{k_n}{\alpha_n}\exp\{-\alpha_n|z-z_0|-ik_n(x-x_0)\} \quad \ldots (25a)$$

$$\phi_2 = -i\frac{Q_h}{2L\mu}\frac{\mu_3-\mu_1}{\mu_1-\mu_2}\frac{1}{\delta_3^2}\sum_{n=-N}^{N}\frac{k_n}{\beta_n}\exp\{-\beta_n|z-z_0|-ik_n(x-x_0)\} \quad \ldots (25b)$$

$$\phi_3 = \operatorname{sgn}(z-z_0)\frac{Q_h}{2L\mu}\frac{1}{\delta_3^2}\sum_{n=-N}^{N}\exp\{-\gamma_n|z-z_0|-ik_n(x-x_0)\}. \quad \ldots (25c)$$

Solving the stress-free boundary conditions at the surface $z = 0$, the wave potentials may be written as

$$\phi_1 = i\frac{\sigma}{\delta_3^2}\sum_{n=-N}^{N}\left\{\frac{\mu_3-\mu_2}{\mu_1-\mu_2}\frac{k_n}{\alpha_n}e^{\alpha_n(z-z_0)}+\frac{G_{1n}}{F_n}e^{-\alpha_n z}\right\}\exp\{-ik_n(x-x_0)\}, \quad \text{... (26a)}$$

$$\phi_2 = -i\frac{\sigma}{\delta_3^2}\sum_{n=-N}^{N}\left\{\frac{\mu_3-\mu_1}{\mu_1-\mu_2}\frac{k_n}{\beta_n}e^{\beta_n(z-z_0)}+\frac{G_{2n}}{F_n}e^{-\beta_n z}\right\}\exp\{-ik_n(x-x_0)\}, \quad \text{... (26b)}$$

$$\phi_3 = -\frac{\sigma}{\delta_3^2}\sum_{n=-N}^{N}\left\{e^{\gamma_n(z-z_0)}+\frac{G_{3n}}{F_n}e^{-\gamma_n z}\right\}\exp\{-ik_n(x-x_0)\}, \quad \text{... (26c)}$$

where

$$G_{1n} = -\ \{(k_n^2+\gamma_n^2)(T_{1n}S_2-T_{2n}S_1) + 4\mu k_n^2\gamma_n(\alpha_n S_2+\beta_n S_1)\}\ \frac{k_n}{\alpha_n}\frac{\mu_3-\mu_2}{\mu_1-\mu_2}e^{-\alpha_n z_0} + \ 8\mu k_n^3\gamma_n S_2\frac{\mu_3-\mu_1}{\mu_1-\mu_2}e^{-\beta_n z_0}+4\mu k_n\gamma_n\{k_n^2+\gamma_n^2\}\ S_2\,e^{-\gamma_n z_0} \quad \text{... (27a)}$$

$$G_{2n} = -\ \{(k_n^2+\gamma_n^2)(T_{1n}S_2-T_{2n}S_1) - 4\mu k_n^2\gamma_n(\alpha_n S_2+\beta_n S_1)\}\ \frac{k_n}{\beta_n}\frac{\mu_3-\mu_1}{\mu_1-\mu_2}e^{-\beta_n z_0} - \ 8\mu k_n^3\gamma_n S_1\frac{\mu_3-\mu_2}{\mu_1-\mu_2}e^{-\alpha_n z_0}+4\mu k_n\gamma_n\{k_n^2+\gamma_n^2\}\ S_1\,e^{-\gamma_n z_0} \quad \text{... (27b)}$$

$$G_{3n} = 4k_n^2(T_{1n}S_2-T_{2n}S_1)\left(\frac{\mu_3-\mu_2}{\mu_1-\mu_2}e^{-\alpha_n z_0}-\frac{\mu_3-\mu_1}{\mu_1-\mu_2}e^{-\beta_n z_0}\right) - (\{T_{1n}S_2-T_{2n}S_1)\}\ \{k_n^2+\gamma_n^2\}\ +\ 4\mu k_n^2\gamma_n(\alpha_n S_2-\beta_n S_1))\,e^{-\gamma_n z_0} \quad \text{... (27c)}$$

and

$$\sigma = \frac{Q_h}{2\mu L}. \quad \text{... (28)}$$

The corresponding displacement components evaluated at $z = 0$, after arranging series for positive index, are given by

$$u_x^0 = \frac{Q_h}{L\mu}\left[(S_1\,\delta_2^2 - S_2\,\delta_1^2)\,\frac{\lambda + 2\mu}{\delta_3^2} \sum_{n=1}^{N} \left\{ 4k_n^2 \left(\frac{\mu_3 - \mu_2}{\mu_1 - \mu_2}\, e^{-\alpha_n z_0} - \frac{\mu_3 - \mu_1}{\mu_1 - \mu_2}\, e^{-\beta_n z_0} \right) \right.\right.$$

$$\left.\left. - 2\left\{ k_n^2 + \gamma_n^2 \right\} e^{-\gamma_n z_0} \right\} \frac{\gamma_n}{F_n} \cos\{k_n (x - x_0)\} - \frac{i}{\delta_3}\, e^{i\delta_3 z_0} \right] \quad \text{... (29)}$$

$$u_z^0 = -\frac{Q_h}{L\mu} \sum_{n=1}^{N} \left\{ 2\left\{ T_{1n}\,S_2 - T_{2n}\,S_1 \right\} \left(\frac{\mu_3 - \mu_2}{\mu_1 - \mu_2}\, e^{-\alpha_n z_0} - \frac{\mu_3 - \mu_1}{\mu_1 - \mu_2}\, e^{-\beta_n z_0} \right) \right.$$

$$\left. - 4\mu\gamma_n \left\{ \alpha_n\,S_2 - \beta_n\,S_1 \right\} e^{-\gamma_n z_0} \right\} \frac{k_n}{F_n} \sin\{k_n (x - x_0)\}. \quad \text{... (30)}$$

Special Cases

In the limiting case of a dry elastic medium (absence of pore fluid) the elastic parameters reduce as :

$$\delta_1^2 = \delta_2^2 = k_\alpha^2\,,\ \delta_3^2 = k_\beta^2\,,\ \alpha_n = \beta_n = \nu_n\,,\ \gamma_n = \gamma_n,\ \text{and}\ \alpha = 0.$$

Hence in an ordinary elastic medium, the horizontal and vertical displacement components are given by :

(i) For a vertical line force

$$u_x^0 = -\frac{Q_v}{\mu L_n} \sum_{n=1}^{N} \frac{k_n}{G_n} \left(4\nu_n\,\gamma_n\, e^{-\nu_n z_0} - 2(k_n^2 + \gamma_n^2)\, e^{-\gamma_n z_0} \right) \sin\ \{k_n (x - x_0)\}$$

$$\text{... (31)}$$

$$u_z^0 = \frac{Q_v}{\mu L} \left\{ -\frac{ik_\alpha}{k_\beta^2}\, e^{-ik_\alpha z_0} + 2 \sum_{n=1}^{N} \frac{\nu_n}{G_n} \left((k_n^2 + \gamma_n^2)\, e^{-\nu_n z_0} - 2k_n^2\, e^{-\gamma_n z_0} \right) \right.$$

$$\left. \times \cos\left\{ k_n (x - x_0) \right\} \right\}. \quad \text{... (32)}$$

(ii) For a horizontal line force

$$u_x^0 = \frac{Q_h}{\mu L} \left\{ -\frac{i}{k_\beta}\, e^{-ik_\beta z_0} - \sum_{n=1}^{N} \frac{\gamma_n}{G_n} \left(4k_n^2\, e^{-\nu_n z_0} - 2(k_n^2 + \gamma_n^2)\, e^{-\gamma_n z_0} \right) \right.$$

$$\left. \times \cos\left\{ k_n (x - x_0) \right\} \right\} \quad \text{... (33)}$$

$$u_z^0 = -\frac{Q_h}{\mu L_n} \sum_{n=1}^{N} \frac{k_n}{G_n} \left(2(k_n^2 + \gamma_n^2)\, e^{-\nu_n z_0} - 4\nu_n\,\gamma_n\, e^{-\gamma_n z_0} \right) \sin\ \{k_n (x - x_0)\}$$

$$\text{... (34)}$$

where k_α, k_β are wave numbers for P and S wave respectively and

$$G_n = (k_n^2 + \gamma_n^2)^2 - 4k_n^2 \nu_n \gamma_n. \qquad \text{... (35)}$$

These results are in accordance with those obtained by Bouchon and Aki[4].

NUMERICAL RESULTS

For simplicity, we assume that the dissipation in the skeletal frame is frequency independent and that it is the same under bulk and shear straining. The anelasticity of the skeletal frame is, hence, approximated by the following complex moduli

$$\lambda = \lambda_0 (1 + i\, 2\xi_s); \;\; \mu = \mu_0 (1 + i\, 2\xi_s),$$

where ξ_s is hysteritic damping and λ_0, μ_0 are the corresponding moduli for ordinary elastic solid.

In order to study the effects of anelasticity and porosity of the solid frame and viscosity of the interstitial fluid on the displacement components, we restrict our numerical work to a particular model. Here, we consider the water saturated sandstone as a fluid saturated porous solid. Following the experimental results given by Yew and Jogi[16], we choose the physical parameters for water saturated sandstone as

$$\lambda_0 = 0.3032 \times 10^{10} \;\; \text{N/m}^2 \qquad \rho = 2.17 \times 10^3 \;\; \text{kg/m}^3$$

$$\mu_0 = 0.922 \times 10^{10} \;\; \text{N/m}^2 \qquad \rho_f = 1.0 \times 10^3 \;\; \text{kg/m}^3$$

$$\delta = 0.738 \times 10^{-10} \;\; (\text{N/m}^2)^{-1} \qquad m = 3.731 \times 10^3 \;\; \text{kg/m}^3$$

$$\gamma = 0.889 \times 10^{-10} \;\; (\text{N/m}^2)^{-1} \qquad \chi = 10^{-11} \;\; \text{m}^2.$$

$$\eta = 3.13 \times 10^{-5} \;\; (\text{N/m}^2) \;\; \text{sec.}$$

Following Biot[2], the Poiseuille flow breaks down if the frequency $f(= \omega/2\pi)$ exceeds a certain value f_t. In case of pores behaving like cylindrical tubes, the frequency is restricted to the range of

$$f < 0.154 \left\{ \frac{\eta}{\chi} \frac{\beta}{2\pi\rho_f} \right\}.$$

In water-saturated sandstone, with above given physical parameters we calculate that the Poiseuille flow breaks down as the frequency f exceeds approximately 20 Hz.

Synthesis is made for 256 frequencies distributed at equal interval for a highest frequency of 20 Hz. Truncation numbers for each of the infinite series {cf. equations (21), (22), (29), (30) and (31)-(34)} are determined numerically by the convergence criterion. The source time dependence assumed is an impulse function $\delta(t)$.

The depth of the source is assumed to be 2 km and the recording device is located at a distance of 10 km from the epicentre. The distance between the sources, L = 65 km, provides enough time to record the disturbance from the single source located at the point (x_0, z_0). For simplicity and to reduce the order of magnitude of displacement, the dimensionless quantity $Q/L\mu_0$ is assmed to be 10^{-6} both for vertical and horizontal line forces. To remove the singularities (in the summations), which would occur at the Rayleigh poles, the imaginary part of the frequency is set to be – 1/40 Hz. The effect of this imaginary part is removed from the final time domain solution. The impulse response is computed from the complex frequency solution by using discrete Fourier transform.

Near-fields are computed for both types of sources : the vertical line force and horizontal line force. Media of propagation of the following types are considered :

(i) Elastic solid half-space; ($\xi_s = 0$).

(ii) Anelastic solid half-space; ($\xi_s = 0.015$).

(iii) Non-dissipative poroelastic solid half-space; $\{\eta/\chi = 0;\ \xi_s = 0\}$.

(iv) Non-dissipative anelastic porous solid half-space $\{\eta/\chi = 0;\ \xi_s = 0.015\}$.

(v) Dissipative poroelastic solid half-space

$$\{\eta/\chi = 3.13 \times 10^6 \text{ N-sec/m}^4;\ \ \xi_s = 0\}.$$

(vi) Dissipative anelastic porous solid half-space

$$\{\eta/\chi = 3.13 \times 10^6 \text{ N-sec/m}^4;\ \ \xi_s = 0.015\}.$$

Discussion of Numerical Results

Using the numerical values given in the previous section, the displacement components (vertical and horizontal) are calculated. With the distance of recording station from the epicenter as 10 kilometers, the first P wave is recorded just after 3 seconds. So all the signals are time shifted by – 3 seconds. In Fig. 1, horizontal displacement due to vertical force is plotted. In this figure four peaks are appearing at the approximate times of 3.2, 3.8, 4.9 and 5.8 seconds, when source is at the distance of 10 kilometers. First and third peak correspond respectively to P and S wave reaching straight from the source to the recording station. Second and fourth peak represent the P and S wave which travels from source to epicenter and then along the surface to recording station. This process is verified and compared by changing the distance between source and recording station to 20 kilometers and shifting the signal by – 6 seconds. Medium considered so far is an ordinary elastic solid half-space.

To observe the effects of porosity, anelasticity and viscosity of the interstitial fluid, displacements are calculated in all the six types of media mentioned in the previous section. Horizontal and vertical displacements due to vertical force are displayed in Figs. 2 and 3 respectively. Corresponding displacement due to horizontal force are presented in figures 4 and 5. It is observed that, with the same elastic

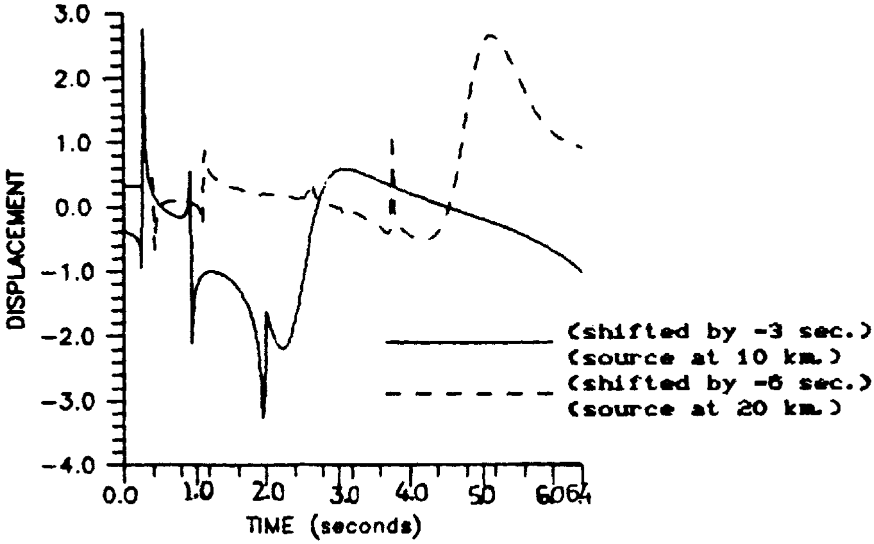

FIG. 1. Effects of source distance on seismogram.

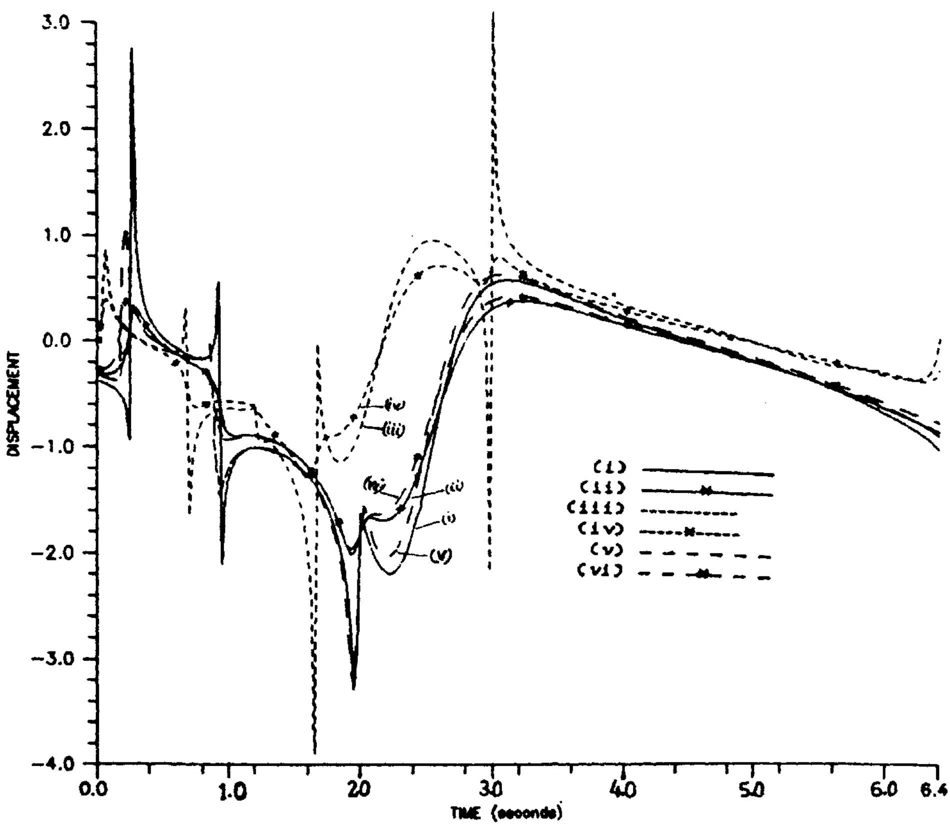

FIG. 2. Seismogram for horizontal displacement due to vertical force.

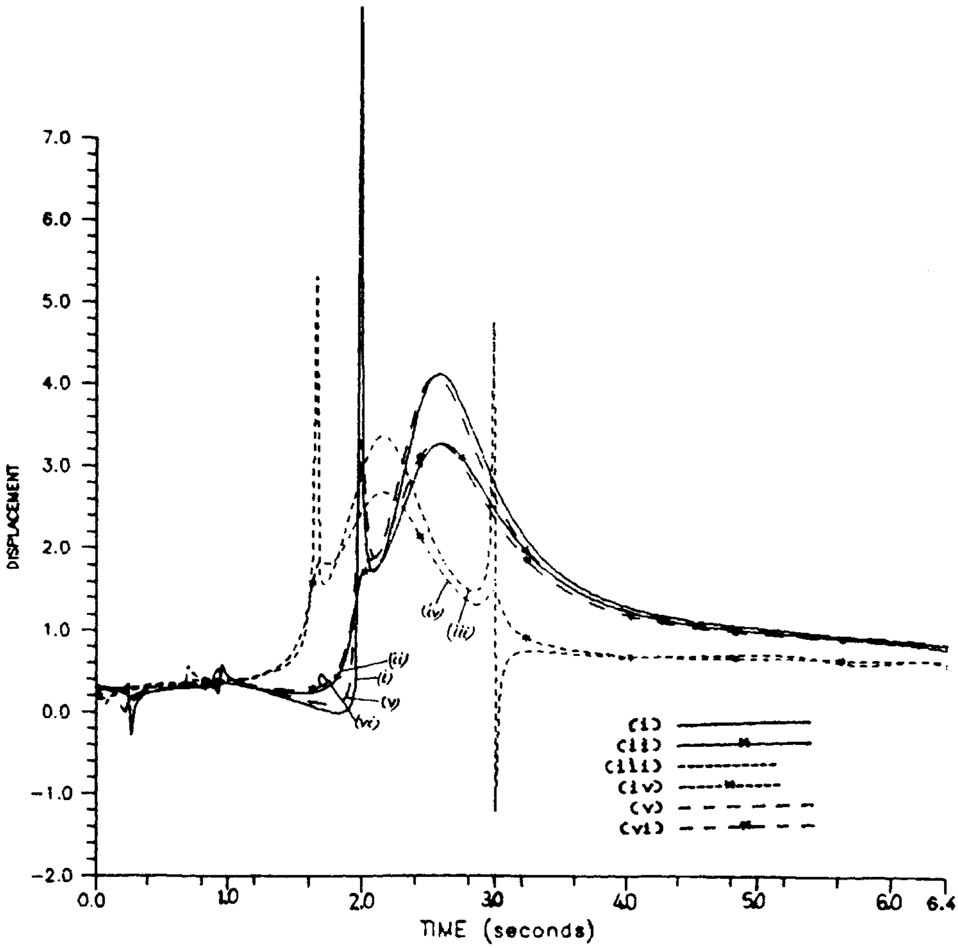

FIG. 3. Seismogram for vertical displacement due to vertical force.

constants of the solid part, waves propagate faster in saturated porous solid than in ordinary elastic solid. Anelasticity of the solid frame decreases the amplitudes of the displacements. In poroelastic solid slow P (or P_S) wave is not much significant except in the case of horizontal force (cf. Fig. 4 and Fig. 5). In this case it appears at about 6.2 seconds, only when poroelastic solid is anelastic. Presence of dissipation due to viscosity of interstitial fluid delays the signal. Also it increases the amplitude of P waves but decreases that of S waves. This being the reason that P_S wave in Fig. 5 is not significant in non-dissipative poroelastic solid but quite clear in dissipative case.

In a non-porous or dry elastic solid, vertical displacement for S waves are much larger than horizontal displacement but for P waves horizontal displacements are

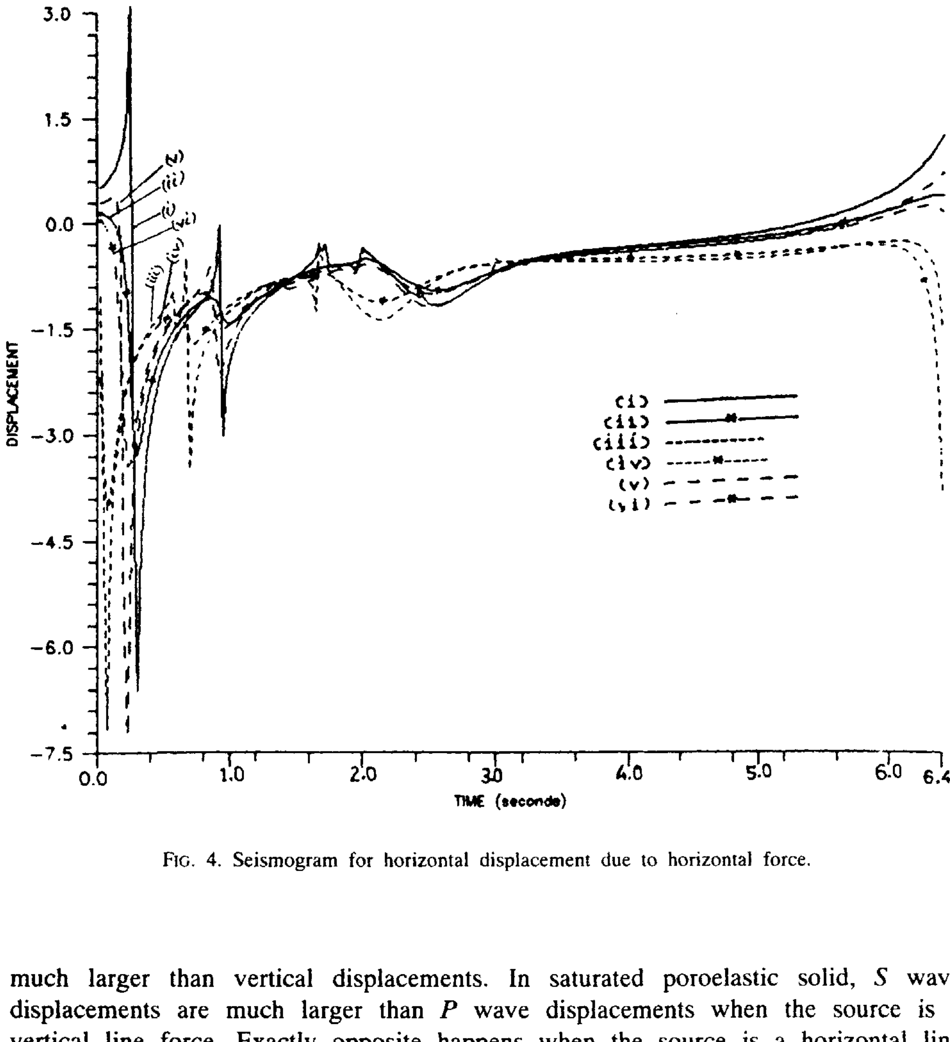

FIG. 4. Seismogram for horizontal displacement due to horizontal force.

much larger than vertical displacements. In saturated poroelastic solid, S wave displacements are much larger than P wave displacements when the source is a vertical line force. Exactly opposite happens when the source is a horizontal line force. In aggregate it is observed that porosity, anelasticity and dissipation have quite significant and well defined effects on the seismograms.

This study considers a more realistic model of earth's crust and hence may help in the near-field studies of more practical sources of strong ground motion. Moreover, this problem calculates the disturbance in the near-field of a source which may help to simulate the data recorded by close-in instruments installed at active faults. The method used calculates the ground motion exactly without any analytical approximation. Assuming the earthquake preparation zone a poroelastic medium, displacements from the active faults can be computed from time to time which may be treated as a useful precursor for a future earthquake. In general it is hoped that this piece of study may be helpful in the further studies, both theoretical and observational, of source problems in fluid saturated porous solids present in the earth.

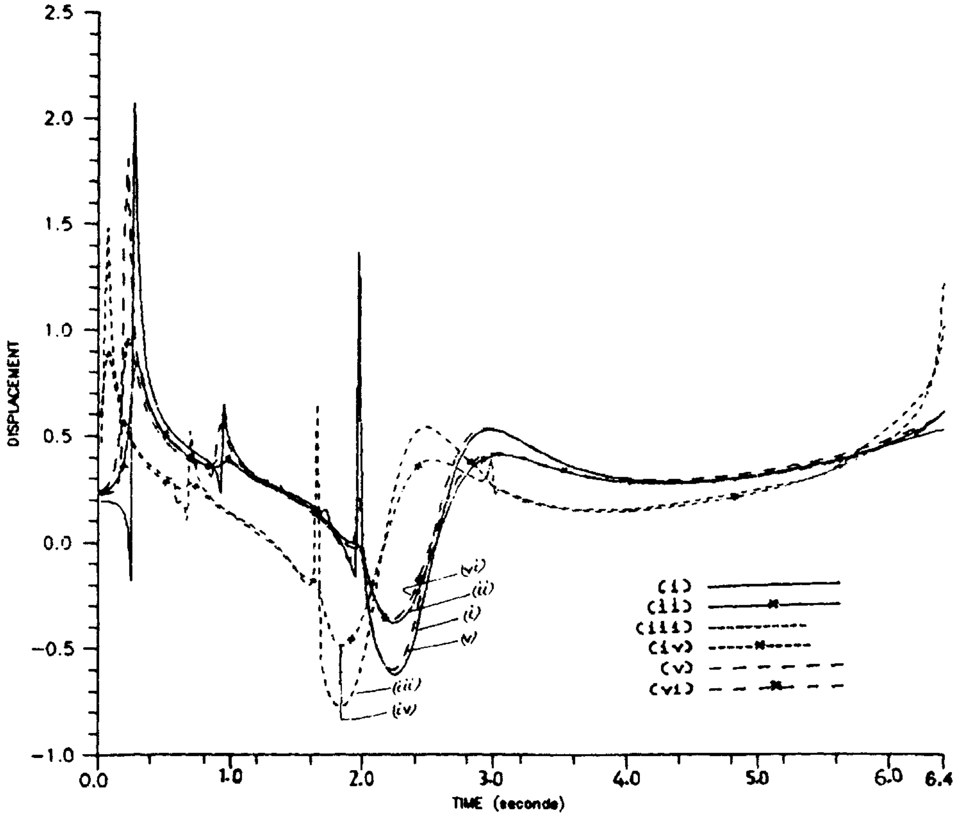

FIG. 5. Seismogram for vertical displacement due to horizontal force.

ACKNOWLEDGEMENT

Authors are thankful to Prof. K. N. Khattri for the idea of this problem. This work was financially supported by CSIR New Delhi (INDIA) in the form of Research Associateship to one of the authors (M.D.S.).

REFERENCES

1. J. L. Aurialt, *Int. J. Engng Sci.* **18** (1980), 775.
2. M. A. Biot, *J. Acoust. Soc. Am.* **28** (1956), 168.
3. M. A. Biot, *J. Appl. Phys.* **33** (1962), 1482.
4. M. Bouchon and K. Aki, *Bull. Seism. Soc. Am.* **67** (1977), 259.
5. C. Boutin, G. Bonnet and P. Y. Bard, *Geophys J. R. Astro. Soc.* **90** (1987), 521.
6. R. Burridge and C. A. Vargas, *Geophys. J. R. Astro. Soc.* **58** (1979), 61.
7. S. Crampin, *First Break* **3** (1985), 12.
8. S. Crampin, *Geophys. J. R. Astro. Soc.* **91** (1987), 331.

9. H. Deresiewicz and R. Skalak, *Bull. Seism. Soc. Am.* **53** (1963), 783.
10. H. Lamb, *Phil. Trans. Roy. Soc. London. Ser. A*, **203** (1904), 1.
11. A. N. Norris, *J. Acoust. Soc. Am.* **77** (1985), 2012.
12. S. Paul, *PAGEOPH* **114** (1976), 605.
13. S. Paul, *PAGEOPH* **114** (1976), 615.
14. A. J. Philippacopoulos, *Bull. Seism. Soc. Am.* **78** (1988), 908.
15. M. D. Sharma, *Bull. Seism. Soc. Am.* **82** (1992), 2263.
16. C. H. Yew and P. N. Jogi, *J. Acoust. Soc. Am.* **60** (1976), 2.